MRS Communications (2015), 5, 251–256
© Materials Research Society, 2015
doi:10.1557/mrc.2015.19

MRS Communications

Polymers/Soft Matter Research Letter

Using tapered interfaces to manipulate nanoscale morphologies in ion-doped block polymers

Wei-Fan Kuan and **Ellen H. Reed†,** Department of Chemical and Biomolecular Engineering, University of Delaware, Newark, Delaware 19716, USA
Ngoc A. Nguyen, Department of Materials Science and Engineering, University of Delaware, Newark, Delaware 19716, USA
Michael E. Mackay and **Thomas H. Epps, III,** Department of Chemical and Biomolecular Engineering, University of Delaware, Newark, Delaware 19716; Department of Materials Science and Engineering, University of Delaware, Newark, Delaware 19716, USA
Address all correspondence to Thomas H. Epps, III at **thepps@udel.edu**

(Received 1 February 2015; accepted 14 April 2015)

Abstract

We detail the influence of tapered interfaces on the nanoscale morphologies of ion-doped poly(styrene-*b*-*oligo*-oxyethylene methacrylate) block polymers (BPs). Most significantly, the location of double-gyroid network phase window was found in ion-doped normal-tapered materials, and a similar window was not detectable in the corresponding non-tapered and inverse-tapered BPs. Additionally, the effective interaction parameters, χ_{eff}, were reduced substantially in the tapered materials in comparison with their non-tapered counterparts. Overall, this work demonstrates that tapering between polymer blocks provides unique control over BP morphologies and improves the material processability (due to lower χ_{eff}), potentially facilitating the development of future ion-conducting devices.

Solid-state polymer electrolytes have become increasingly attractive for lithium-based battery applications as they exhibit low volatility, provide sufficient mechanical strength, and increase the thermal and electrochemical stability of batteries in comparison to conventional liquid electrolytes that use flammable organic solvents.[1,2] Among the various macromolecular architectures of polymer electrolytes, block polymers (BPs) are of particular interest due to their ability to self-assemble into ordered nanostructures such as lamellae (LAM), hexagonally packed cylinders (HEX), body-centered cubic spheres (BCC), and double-gyroid (DG) networks.[3–5] A number of studies have shown that BP nanostructures, which are governed by the segregation strength (χN, χ: Flory–Huggins interaction parameter and N: degree of polymerization) and volume fraction (f) of the block, can form well-defined conducting pathways, which leads to enhanced ionic conductivities in comparison to corresponding random copolymers.[6,7] Of the more common BP nanostructures, the DG network phase is one of the most appealing due to its three-dimensional (3D) domain connectivity.[8] A 3D continuous morphology allows each domain to contribute directly to the modulus of the material, which leads to improvements in toughness, stress at break, and high-temperature creep resistance;[9,10] thus, a network morphology is desirable from a mechanical property perspective. Additionally, network morphologies can form 3D conducting pathways, which enhances ion transport in battery electrolyte membranes without costly and time-consuming alignment procedures that may be necessary for 1D and 2D nanostructures.[11–15] These advantages make BP networks promising candidates for potential conducting applications.

However, the design of network-forming polymer electrolytes is complicated by the relatively narrow network composition windows in the BP phase diagram, especially at high effective segregation strengths ($\chi_{eff}N$).[3] As one avenue to overcome this limitation, recent efforts on tapered block polymers (TBPs) are noteworthy.[16,17] TBPs are a class of BPs with well-defined and synthetically controlled interfacial regions that taper from one polymer block to another. A common example used in this work is shown in Fig. 1(a). Previous studies have reported that incorporating a tapered region between pure blocks in a copolymer can decrease the effective segregation strength by reducing χ_{eff};[18,19] in other words, BP thermal morphology transitions may be tuned independent of the chemical constituents and molecular mass using tapered interfaces. Moreover, theoretical work by Hall and co-workers demonstrated that the normal-tapered interface in BPs can relieve some of the packing frustration inherent in the DG morphology, thus widening the network phase window and increasing the propensity to generate network structures.[20] Therefore, TBPs offer exciting potential for creating novel polymer electrolytes with complex co-continuous nanostructures.

In this work, we systematically investigated the phase behavior of lithium ion-doped tapered and non-tapered BPs based on poly (styrene-*b*-*oligo*-oxyethylene methacrylate) [P(S-OEM)] over a

† Current address: Department of Chemical and Biomolecular Engineering, University of Pennsylvania, Philadelphia, Pennsylvania 19104.

https://doi.org/10.1557/mrc.2015.19 Published online by Cambridge University Press

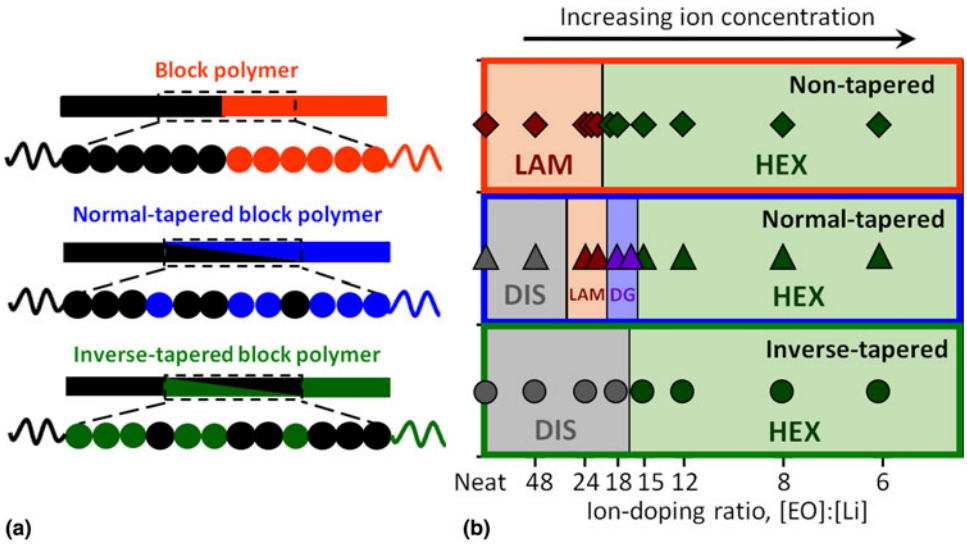


Figure 1. (a) Illustration of non-tapered, normal-tapered, and inverse-tapered BPs. (b) Phase behavior of non-tapered P(S-OEM), normal-tapered P(S-SOEM-OEM), and inverse-tapered P(S-OEMS-OEM) BPs as a function of the ion-doping ratio. LAM, lamellae; HEX, hexagonally packed cylinders; DIS, disordered phase; DG, double gyroid.

range of ion-doping ratios. The polymers were synthesized *via* atom transfer radical polymerization and doped with lithium trifluoromethanesulfonate (lithium triflate, $LiCF_3SO_3$) as described elsewhere.[21] The normal-tapered and inverse-tapered interfaces between blocks were generated through a semi-batch feed approach using programmable syringe pumps. All polymers had consistent number-average molar masses ($M_n \approx 33$ kg/mol) and overall polymer compositions ($f_{POEM} \approx 0.52$); see Table S1 in Supplementary Material. Both the normal-tapered and inverse-tapered BPs had a taper volume fraction of ≈ 0.6. The associated phase behavior is illustrated in Fig. 1(b). Over the experimental range of salt-doping levels, the non-tapered samples exhibited a transition from LAM to HEX, while the inverse-tapered BPs showed a transition from a disordered morphology (DIS) to HEX. Interestingly, the normal-tapered materials demonstrate an increase in the richness of phase behavior, sampling several morphologies including the desirable DG network. Thus, it is evident that the tapered interfaces significantly influence the phase behavior of ion-doped BPs.

The morphologies of all polymers were identified via small-angle X-ray scattering (SAXS) performed on the DND-CAT 5-ID-D beamline at the Advanced Photon Source (APS, Argonne National Laboratory). SAXS traces of non-tapered, normal-tapered, and inverse-tapered BPs as a function of ion-doping ratio ([EO]:[Li]) are shown in Fig. 2. In all cases, as the lithium ion concentration increases, the primary scattering peak location (q^*) shifts to smaller q values, indicating larger domain spacings ($d = 2\pi/q^*$). This shift is expected as ion-doping previously has been shown to induce polymer chain stretching.[22] Additionally, primary diffraction peaks of the ion-doped polymers appear to broaden at the higher ion concentrations ([EO]:[Li] = 8:1 and 6:1). This broadening may be attributed to a combination of higher segregation strength and the transient crosslinking between lithium ions and unpaired electrons on the oxygen atoms in POEM block.[23] These two factors may reduce polymer chain mobility or ordering kinetics. In Fig. 2(a), the non-tapered P(S-OEM) samples with neat (non-doped), 48:1, and 24:1 ion-doping ratios exhibit a LAM morphology with observed SAXS reflections at $q/q^* = 1$, 2, and 3, whereas the samples with ion-doping ratios from 18:1 to 6:1 display HEX structures with observed SAXS reflections at $q/q^* = 1, \sqrt{3}, 2, \sqrt{7}$, and 3.[22] Three additional ion-doped P(S-OEM) samples ([EO]:[Li] = 22:1, 20:1, and 19:1) were prepared to examine the BP morphologies between 24:1 and 18:1 ion-doping ratios. The corresponding SAXS patterns (see Fig. S1 in Supplementary Material) indicate that the LAM-to-HEX phase transition occurs between 20:1 and 19:1 ion-doping levels in the non-tapered BP.

In Fig. 2(b), the SAXS patterns for normal-tapered P(S-SOEM-OEM) demonstrate a disordered morphology at neat and 48:1 ion-doping ratios, whereas the non-tapered P(S-OEM) exhibits a lamellar morphology at the same ion-doping ratios. As both samples have a similar molecular mass and overall composition, this difference in morphology likely is a result of the reduction in χ_{eff} for the TBPs. Upon the addition of lithium salt to a doping ratio of 24:1, the primary peak narrows noticeably [Fig. 2(b)], suggesting a transition to an ordered nanostructure occurs between [EO]:[Li] = 48:1 and 24:1. The ordered phase in the 24:1 ion-doped P(S-SOEM-OEM) sample, as indicated by the SAXS peaks at $q/q^* = 1$ and 2, likely is LAM. More significantly, P(S-SOEM-OEM) with an 18:1 ion-doping ratio exhibits diffraction peaks at $q/q^* = \sqrt{6}, \sqrt{8}, \sqrt{14}$, and $\sqrt{22}$. With the primary peak corresponding to $q^*\sqrt{6}$ ($q^* = q_{112}$), the relative peak ratios suggest a DG

https://doi.org/10.1557/mrc.2015.19 Published online by Cambridge University Press

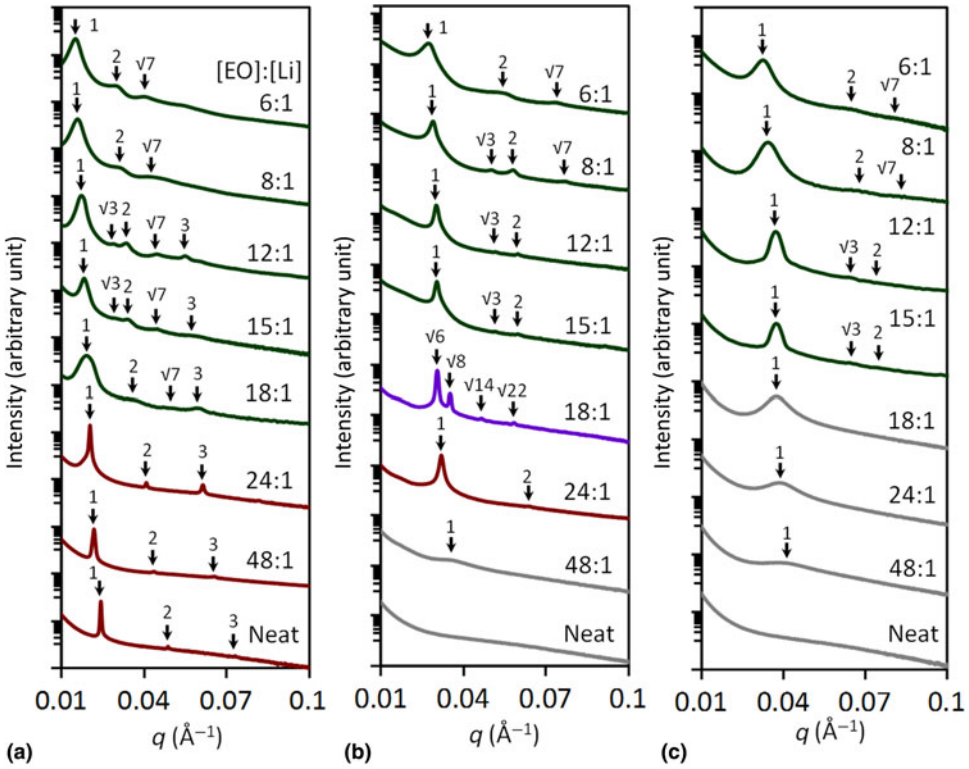


Figure 2. SAXS profiles for (a) P(S-OEM), (b) P(S-SOEM-OEM), and (c) P(S-OEMS-OEM) with various ion-doping ratios at 120 °C. The relative peak ratios (q/q^*) are indicated by arrows, and the phase assignment is color-coded: red, LAM; green, HEX; gray, DIS; purple, DG. All SAXS samples were pre-annealed at 120 °C for 2 h, heated to 150 °C for 2 h, and then cooled to 30 °C, all under dynamic vacuum. Data are shifted vertically for clarity.

network morphology.[13,24] This nanostructure was stable during thermal annealing from 30 to 150 °C. To probe the breadth of the DG phase region, two additional ion-doped normal-tapered samples, [EO]:[Li] = 20:1 and 16:1, were prepared. Although the P(S-SOEM-OEM) sample at a 20:1 ion-doping ratio exhibits a LAM morphology, the 16:1 sample retains the DG network phase (see Fig. S2 in Supplementary Material). This finding indicates that a DG network phase window was generated in the ion-doped TBP system even though no DG morphology was detected in the non-tapered P(S-OEM) BPs at a similar composition over the experimental range of doping ratios. At higher ion concentrations (from [EO]:[Li] = 15:1 to 6:1), P(S-SOEM-OEM) samples show SAXS reflections at $q/q^* = 1$, $\sqrt{3}$, 2, and $\sqrt{7}$, which are consistent with HEX structures and similar to the nanostructures at higher ion concentrations in the ion-doped P(S-OEM) system.

For the inverse-tapered P(S-OEMS-OEM), the $LiCF_3SO_3$-doped polymers retain a disordered morphology from neat (no-salt) to 18:1, and the polymers form a HEX morphology at higher ion concentrations [Fig. 2(c) and Fig. S3]. The expanded disordered phase window (from neat to 18:1 instead of from neat to 48:1 in the normal-tapered material) is expected as the inverse-tapered interfaces are suspected to have a greater ability to increase block compatibility (i.e. lowering of order–disorder transition temperatures) relative to their normal-tapered analogs.[17,20,25]

Transmission electron microscopy (TEM, JEM-3010) and dynamic mechanical analysis (DMA, ARES-G2 rheometer, TA Instruments) also were used to characterize the self-assembly of ion-doped tapered and non-tapered BPs. The experiments were performed on samples with ion-doping ratios of 18:1, in which the three polymers exhibited different morphologies according to the SAXS data. One can see in the TEM micrograph of $LiCF_3SO_3$-doped P(S-OEM) [Fig. 3(a)] that there are parallel stripes and hexagonally packed dots, supporting a HEX assignment. The TEM micrograph for $LiCF_3SO_3$-doped P(S-SOEM-OEM) in Fig. 3(b) displays the "wagon-wheel" [111] projection, which is characteristic of DG network structures.[8,17,24] The TEM micrograph given in Fig. 3(c) lacks obvious ordering, suggesting a disordered morphology for the inverse-tapered P(S-OEMS-OEM).

The isothermal frequency sweep analysis for all three ion-doped polymers at [EO]:[Li] = 18:1 is shown in Fig. 3(d). Linear dynamic shear moduli of BP melts strongly are influenced by the morphology in the terminal response regime (low-frequency region), in which the storage modulus follows a power-law relationship to frequency ($G' \propto \omega^a$; G' is the storage modulus, and ω is the frequency).[26] The power-law exponent,

https://doi.org/10.1557/mrc.2015.19 Published online by Cambridge University Press

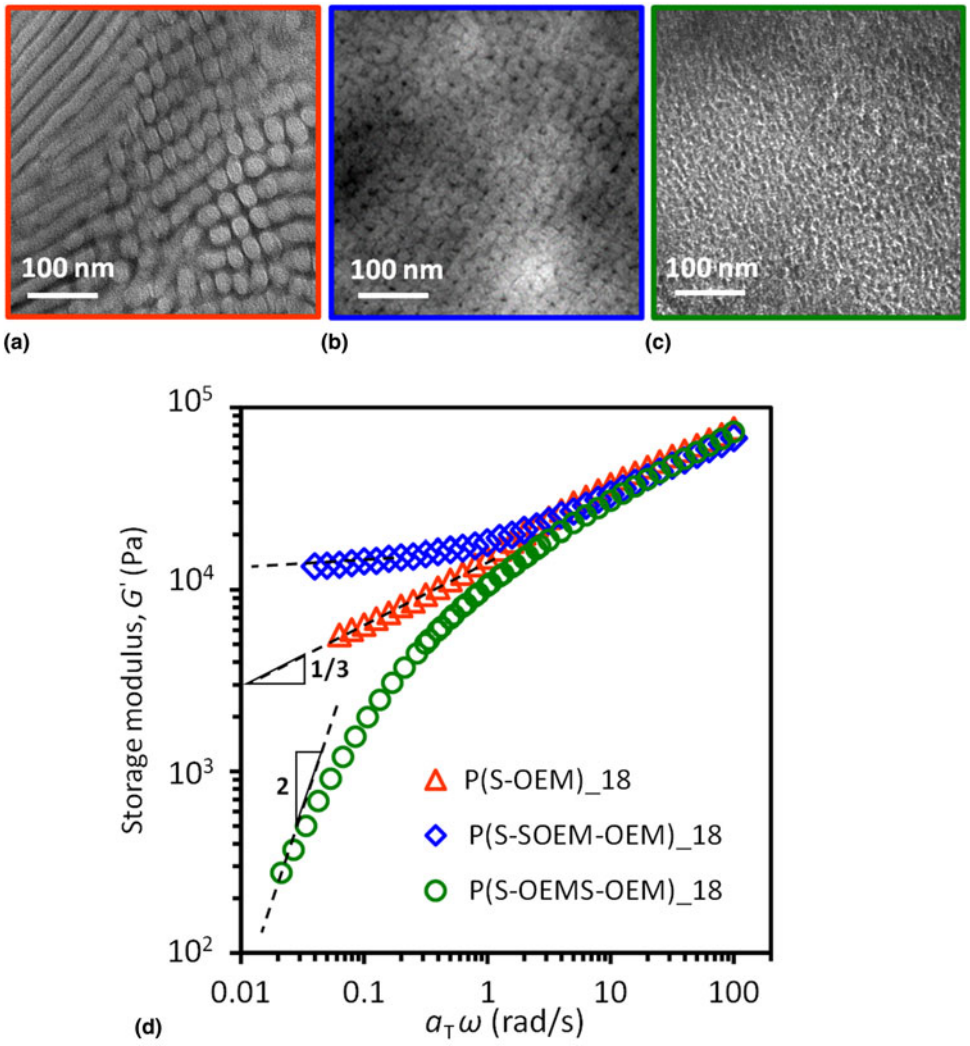


Figure 3. TEM images for $LiCF_3SO_3$-doped polymers at [EO]:[Li] = 18:1: (a) P(S-OEM); (b) P(S-SOEM-OEM); (c) P(S-OEMS-OEM). TEM specimens were cut into ≈70 nm slices from the thermally annealed SAXS samples at −120 °C on a cryo-microtome. The POEM domains were stained preferentially with RuO_4 vapor to enhance domain contrast prior to imaging. (d) Isothermal frequency sweeps for 18:1 $LiCF_3SO_3$-doped P(S-OEM) at 110 °C and 18:1 $LiCF_3SO_3$-doped TBPs. DMA results for both TBPs were shifted according to time–temperature superposition using a reference temperature of 70 °C. 8 mm diameter parallel plates were utilized for the DMA experiments. Data were collected at a strain of 3%. Dash lines are included for visual clarity of the terminal responses. The number in the legend represents the [EO]:[Li] ion-doping ratio for the sample. The brightness in (c) was enhanced for visual clarity.

a, ranges from 0 for an elastic solid to 2 for a disordered melt.[26] The DMA data for $LiCF_3SO_3$-doped P(S-OEM) presents a terminal response with $G' \propto \omega^{1/3}$, in which the exponent of 1/3 is indicative of a HEX morphology.[26] For $LiCF_3SO_3$-doped P(S-SOEM-OEM), G' approaches a plateau as the frequency is decreased. This nearly frequency-independent behavior is a solid-like response that suggests triply periodic structures,[26,27] further supporting a DG phase assignment. For $LiCF_3SO_3$-doped P(S-OEMS-OEM), the modulus obeys a power law of $G' \propto \omega^2$ in the low-frequency region. This scaling behavior suggests a disordered phase for P(S-OEMS-OEM) at [EO]:[Li] = 18:1. Both TEM and DMA results are consistent with the morphological characterization data from SAXS. The combination of SAXS, TEM, and DMA strongly indicates that the tapered interfaces present an efficient method for manipulating the morphologies of ion-doped BPs at constant molecular mass and chemical composition.

To further explore the influence of tapered interfaces on BP phase behavior, χ_{eff} values between pure blocks in non-tapered, normal-tapered, and inverse-tapered BP systems were estimated using random phase approximation (RPA) theory (see Supplementary Material for details).[28–30] The temperature dependence of χ_{eff} for the neat and $LiCF_3SO_3$-doped polymers is summarized in Fig. 4. It is important to note that, because the RPA approach for calculating χ_{eff} requires disordered samples, the window over which χ_{eff} can be evaluated narrows rapidly

https://doi.org/10.1557/mrc.2015.19 Published online by Cambridge University Press

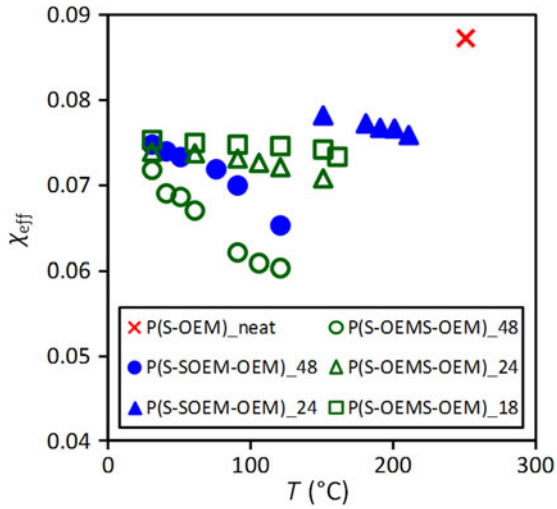


Figure 4. Temperature dependence of χ_{eff} for disordered P(S-OEM), P(S-SOEM-OEM), and P(S-OEMS-OEM). The number in the legend represents the [EO]:[Li] ion-doping ratio for the sample.

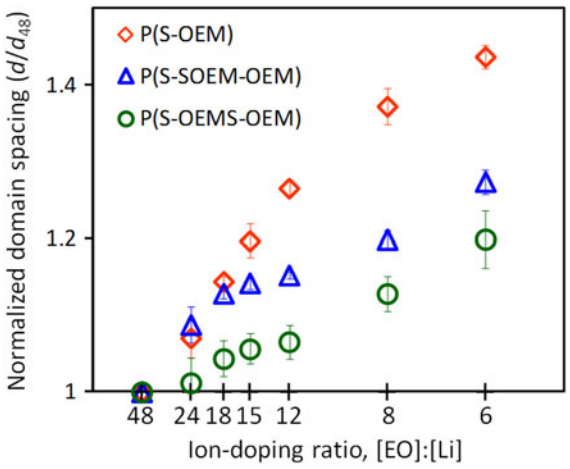


Figure 5. Normalized domain spacings as a function of ion-doping ratio for P(S-OEM), P(S-SOEM-OEM), and P(S-OEMS-OEM). d_{48} represents the domain spacing of each polymer at [EO]:[Li] = 48:1. Error bars are standard deviations from the SAXS data. For comparison purposes, the normalized domain spacing of the DG-forming P(S-SOEM-OEM), [EO]:[Li] = 18:1, was using $d = 2\pi/(q^* \sqrt{6})$.

with increasing ion concentration. Additionally, as neat P(S-SOEM-OEM) and P(S-OEMS-OEM) samples exhibit nearly featureless SAXS patterns [Figs. 2(b) and 2(c)], the fitting of χ_{eff} for neat TBPs is not appropriate. The increase of ion concentration in TBPs as shown in Fig. 4, from [EO]:[Li] = 48:1 to 24:1, leads to the increase in χ_{eff} between two block components. Also, the normal-tapered materials, in both 48:1 and 24:1 ion-doping ratios, exhibit higher χ_{eff} values in comparison to inverse-tapered analogs, again suggesting the enhanced block compatibility of inverse-taper relative to the normal-taper. Most importantly, the neat P(S-OEM) sample displays the largest χ_{eff} among all polymers in Fig. 4, demonstrating that tapered interfaces significantly reduced polymer–polymer interactions between blocks, especially for the inverse-tapered materials. This reduction in χ_{eff} can lead to lower order–disorder transition temperatures, improving materials processability by decreasing processing temperatures and potential solvent usage.

The normalized domain spacing data (d/d_{48}, in which d_{48} is the domain spacing of the corresponding polymer at an ion-doping ratio of 48:1) for polymers at various ion-doping ratios is given in Fig. 5. (The domain spacing of each sample can be found in Table S2.) The domain spacing of the BPs was calculated using the primary peak location from the SAXS patterns in Fig. 2. In all cases, the normalized domain spacing increases as the ion concentration increases. For the majority of the ion-doping ratios, the normalized domain spacings of $LiCF_3SO_3$-doped P(S-OEM) materials are larger than those of $LiCF_3SO_3$-doped TBPs, especially in comparison to the inverse-tapered P(S-OEMS-OEM) system. As all three samples are of comparable molecular mass and composition, the smaller domain spacing changes in TBPs most likely are caused by the presence of the tapered interfaces. Similar domain spacing behavior was suggested by Hall and co-workers using self-consistent field theory calculation.[20] The Hall work on TBP domain spacings demonstrated that different chain conformations at the block interface could impact the polymer chain stretching at increasing χN, which is consistent with the findings herein.

In summary, the self-assembly of lithium ion-doped P(S-OEM) BPs and TBPs exhibits a strong dependence on the presence of tapered interfaces, the profile of the tapers (normal or inverse), and the concentration of lithium ions. Of particular importance is the experimental discovery of a DG network phase window in the ion-doped, normal-tapered system despite the fact that no network morphologies were detected in the non-tapered and inverse-tapered materials. Moreover, this work shows that tapered interfaces present a promising strategy for reducing the polymer–polymer interactions and polymer chain stretching upon lithium ion addition. The results highlighted herein suggest an advanced design pathway for the next generation of nanostructured and highly processable materials in transport applications.

Supplementary materials

For supplementary material for this article, please visit http://dx.doi.org/10.1557/mrc.2015.19

Acknowledgments

We gratefully acknowledge AFOSR-PECASE (FA9550-09-1-0706) and National Science Foundation (DMR-1207041) for financial support. N. A. Nguyen was supported by NIST (grant no. 70NANOBIOH256) and funding provided through the Department of Materials Science and Engineering at UD. This research used resources of the Advanced Photon Source, a U.S. Department of Energy (DOE) Office of Science User

https://doi.org/10.1557/mrc.2015.19 Published online by Cambridge University Press

Facility operated for the DOE Office of Science by Argonne National Laboratory under Contract No. DE-AC02-06CH11357. We thank the W. M. Keck Electron Microscopy Facility at UD for use of their TEM and cryo-microtome facilities. This publication was made possible by the Delaware COBRE program, supported by a grant from the National Institute of General Medical Sciences – NIGMS (1 P30 GM110758-01) from the National Institutes of Health.

References

1. W.-S. Young, W.-F. Kuan, and T.H. Epps, III: Block copolymer electrolytes for rechargeable lithium batteries. *J. Polym. Sci. B: Polym. Phys.* **52**, 1 (2014).
2. D.T. Hallinan and N.P. Balsara: Polymer electrolytes. *Annu. Rev. Mater. Res.* **43**, 503 (2013).
3. M.W. Matsen: Effect of architecture on the phase behavior of AB-type block copolymer melts. *Macromolecules* **45**, 2161 (2012).
4. H. Hu, M. Gopinadhan, and C.O. Osuji: Directed self-assembly of block copolymers: a tutorial review of strategies for enabling nanotechnology with soft matter. *Soft Matter* **10**, 3867 (2014).
5. J.M. Widin, A.K. Schmitt, A.L. Schmitt, K. Im, and M.K. Mahanthappa: Unexpected consequences of block polydispersity on the self-assembly of ABA triblock copolymers. *J. Am. Chem. Soc.* **134**, 3834 (2012).
6. Y. Ye, S. Sharick, E.M. Davis, K.I. Winey, and Y.A. Elabd: High hydroxide conductivity in polymerized ionic liquid block copolymers. *ACS Macro Lett.* **2**, 575 (2013).
7. P.P. Soo, B. Huang, Y.I. Jang, Y.M. Chiang, D.R. Sadoway, and A.M. Mayes: Rubbery block copolymer electrolytes for solid-state rechargeable lithium batteries. *J. Electrochem. Soc.* **146**, 32 (1999).
8. A.J. Meuler, M.A. Hillmyer, and F.S. Bates: Ordered network mesostructures in block polymer materials. *Macromolecules* **42**, 7221 (2009).
9. B.J. Dair, C.C. Honeker, D.B. Alward, A. Avgeropoulos, N. Hadjichristidis, L.J. Fetters, M. Capel, and E.L. Thomas: Mechanical properties and deformation behavior of the double gyroid phase in unoriented thermoplastic elastomers. *Macromolecules* **32**, 8145 (1999).
10. H. Pernot, M. Baumert, F. Court, and L. Leibler: Design and properties of co-continuous nanostructured polymers by reactive blending. *Nat. Mater.* **1**, 54 (2002).
11. W.-S. Young and T.H. Epps, III: Ionic conductivities of block copolymer electrolytes with various conducting pathways: sample preparation and processing considerations. *Macromolecules* **45**, 4689 (2012).
12. B.K. Cho, A. Jain, S.M. Gruner, and U. Wiesner: Mesophase structure-mechanical and ionic transport correlations in extended amphiphilic dendrons. *Science* **305**, 1598 (2004).
13. G. Jo, H. Ahn, and M.J. Park: Simple route for tuning the morphology and conductivity of polymer electrolytes: one End functional group is enough. *ACS Macro Lett.* **2**, 990 (2013).
14. I. Villaluenga, X.C. Chen, D. Devaux, D.T. Hallinan, and N.P. Balsara: Nanoparticle-driven assembly of highly conducting hybrid block copolymer electrolytes. *Macromolecules* **48**, 358 (2015).
15. R.L. Weber, Y.S. Ye, A.L. Schmitt, S.M. Banik, Y.A. Elabd, and M.K. Mahanthappa: Effect of nanoscale morphology on the conductivity of polymerized ionic liquid block copolymers. *Macromolecules* **44**, 5727 (2011).
16. W.-F. Kuan, R. Roy, L. Rong, B.S. Hsiao, and T.H. Epps, III: Design and synthesis of network-forming triblock copolymers using tapered block interfaces. *ACS Macro Lett.* **1**, 519 (2012).
17. R. Roy, J.K. Park, W.-S. Young, S.E. Mastroianni, M.S. Tureau, and T.H. Epps, III: Double-gyroid network morphology in tapered diblock copolymers. *Macromolecules* **44**, 3910 (2011).
18. T. Pakula and K. Matyjaszewski: Copolymers with controlled distribution of comonomers along the chain .1. Structure, thermodynamics and dynamic properties of gradient copolymers. Computer simulation. *Macromol. Theory Simul.* **5**, 987 (1996).
19. P. Hodrokoukes, G.A. Floudas, S. Pispas, and N. Hadjichristidis: Microphase separation in normal and inverse tapered block copolymers of polystyrene and polyisoprene. 1. Phase state. *Macromolecules* **34**, 650 (2001).
20. J.R. Brown, S.W. Sides, and L.M. Hall: Phase behavior of tapered diblock copolymers from self-consistent field theory. *ACS Macro Lett.* **2**, 1105 (2013).
21. W.-F. Kuan, R. Remy, M.E. Mackay, and T.H. Epps, III: Controlled ionic conductivity via tapered block polymer electrolytes. *RSC Adv.* **5**, 12597 (2015).
22. W.-S. Young and T.H. Epps, III: Salt doping in PEO-containing block copolymers: counterion and concentration effects. *Macromolecules* **42**, 2672 (2009).
23. T.H. Epps, III, T.S. Bailey, H.D. Pham, and F.S. Bates: Phase behavior of lithium perchlorate-doped Poly(styrene-b-isoprene-b-ethylene oxide) triblock copolymers. *Chem. Mater.* **14**, 1706 (2002).
24. M.S. Tureau and T.H. Epps, III: Effect of partial hydrogenation on the phase behavior of Poly(isoprene-b-styrene-b-methyl methacrylate) triblock copolymers. *Macromolecules* **45**, 8347 (2012).
25. N. Singh, M.S. Tureau, and T.H. Epps, III: Manipulating ordering transitions in interfacially modified block copolymers. *Soft Matter* **5**, 4757 (2009).
26. M.B. Kossuth, D.C. Morse, and F.S. Bates: Viscoelastic behavior of cubic phases in block copolymer melts. *J. Rheol.* **43**, 167 (1999).
27. M.S. Tureau and T.H. Epps, III: Nanoscale networks in poly[isoprene-block-styrene-block-(methyl methacrylate)] triblock copolymers. *Macromol. Rapid Commun.* **30**, 1751 (2009).
28. S. Naidu, H. Ahn, J. Gong, B. Kim, and D.Y. Ryu: Phase behavior and ionic conductivity of lithium perchlorate-doped polystyrene-b-poly(2-vinylpyridine) copolymer. *Macromolecules* **44**, 6085 (2011).
29. L. Leibler: Theory of microphase separation in block copolymers. *Macromolecules* **13**, 1602 (1980).
30. A.A. Teran and N.P. Balsara: Thermodynamics of block copolymers with and without salt. *J. Phys. Chem. B* **118**, 4 (2013).

https://doi.org/10.1557/mrc.2015.19 Published online by Cambridge University Press